Medicinal Chemistry Research
https://doi.org/10.1007/s00044-019-02434-1

MEDICINAL CHEMISTRY RESEARCH

ORIGINAL RESEARCH

Synthesis, structural characterization, and cytotoxic evaluation of chalcone derivatives

Paulo N. Bandeira[1] · Telma L. G. Lemos[2] · Hélcio S. Santos[1,3] · Mylena C. S. de Carvalho[4] · Daniel P. Pinheiro[4] · Manoel O. de Moraes Filho[4] · Cláudia Pessoa[4,5] · Francisco W. A. Barros-Nepomuceno[6] · Tigressa H. S. Rodrigues[1] · Paulo R. V. Ribeiro[7] · Herbert S. Magalhães[2] · Alexandre M. R. Teixeira[3]

Received: 16 March 2019 / Accepted: 28 August 2019

Abstract

Chalcones containing amino or acetamide groups on ring A and electron donating/withdrawing groups on ring B have been shown to have great cytotoxic potential against human cancer cell lines. In this work, a series of twenty chalcones, including nine 1-(4′-aminophenyl)-3-(substituted aryl)-2-propen-1-ones (**1**–**9**), nine 1-(4′-acetamidophenyl)-3-(substituted aryl)-2-propen-1-ones (**1a**–**9a**), and two 1-(3′-methoxy-4′-hydroxyphenyl)-3-(substituted aryl)-2-propen-1-ones (**10**, **11**), were synthesized and submitted for initial biological screening using HCT-116 cells. Among the evaluated compounds, chalcone **6a** showed strong and selective activity against HCT-116 cells ($IC_{50} = 2.37 \pm 0.73$ μM). The preliminary structure–activity relationship analysis indicated that the cytotoxic effect of these compounds might be attributed to the combined effect of two electron withdrawing groups: the nitro group (NO_2) at the *meta*-position of ring B and the acetyl group at the *para*-position of ring A. Moreover, chalcone **6a** was able to induce G2/M cell cycle arrest and apoptosis at a concentration of 10 μM after 24 h of incubation. These data reinforce that compound **6a** could be a promising lead compound for the future exploration of selective anti-colon carcinoma cancer agents.

Keywords Synthesis · NMR · Infrared · Chalcone · 4′-acetamidochalcones · Cytotoxic activity

Introduction

Chalcones are open chain flavonoids that are characterized by two aromatic rings joined by a three-carbon α, β-unsaturated carbonyl system (Fig. 1). These compounds can be isolated from natural sources due to their widespread distribution in fruits, vegetables, and tea or they can be synthesized by chemical processes (Abbas et al. 2014; Di Carlo et al. 1999).

Over the last several years, chalcones have instigated the interest of chemical and pharmacological researchers due to their simple chemical structure and varied biological activities. The chalcone biological activity spectrum includes antinociceptive, anti-inflammatory (Padaratz et al. 2009; Corrêa et al. 2001; De Campos-Buzzi et al. 2007; Nowakowska 2007; de Campos-Buzzi et al. 2006), anti-tumor (Zingales and Moore 2016; Cabrera et al. 2007), antibacterial, antifungal (Karaman et al. 2010), anti-leishmanial (Boeck et al. 2006), and antioxidant activity (Prasad et al. 2013). This wide range of activity is mainly due to the numerous substitution possibilities on the chalcone aromatic rings. Moreover, the synthesis of chalcones

Supplementary information The online version of this article (https://doi.org/10.1007/s00044-019-02434-1) contains supplementary material, which is available to authorized users.

✉ Alexandre M. R. Teixeira
amrteixeira@gmail.com

1 Curso de Química, Universidade Estadual Vale do Acaraú, Sobral, CE, Brazil

2 Departamento de Química Orgânica e Inorgânica, Universidade Federal do Ceará, Fortaleza, CE, Brazil

3 Departamento de Química Biológica, Universidade Regional do Cariri, Crato, CE, Brazil

4 Núcleo de Pesquisa e Desenvolvimento de Medicamentos, Universidade Federal do Ceará, Fortaleza, CE, Brazil

5 Fundação Oswaldo Cruz, FIOCRUZ-CE, Eusebio, CE, Brazil

6 Instituto de Ciências da Saúde, Universidade da Integração Internacional da Lusofonia Afro-Brasileira, Acarape, CE, Brazil

7 Laboratório Multiusuário de Química de Produtos Naturais, Embrapa Agroindústria Tropical, Fortaleza, CE, Brazil

Published online: 06 September 2019

based on the Claisen–Schmidt condensation reaction allows a vast number of compounds to be obtained, providing the desired structural variety (Ducki et al. 1998).

There is a continuous scientific effort that has been expended on the design and development of anticancer chalcones that has resulted in many novels and chemically diverse chalcones with therapeutic potential against different types of cancer (Karthikeyan et al. 2015). In this context, chalcones are able to induce cell cycle arrest and apoptosis in various human cancer cell lines. These abilities can be attributed, in part, by tubulin polymerization inhibition and/or the capacity to bind at the DNA minor groove of neoplastic cells. The antimetastatic potential and antiangiogenic actions are related to flavokawain B, a chalcone isolated from the root extracts of kava-kava plants (Lindamulage et al. 2017; Hassan et al. 2017; Shankaraiah et al. 2017; Rossette et al. 2017).

Recent studies have shown the cytotoxic anticancer potential of chalcones that contain an amino or acetamide group on ring A (Santos et al. 2017; Jardim et al. 2015; Tristão et al. 2012.). Chalcones with hydroxyl, methoxy, and halogen groups on the B ring have also presented effective cytotoxic potential against human cancer cell lines (Karthikeyan et al. 2015). Based on this information, chalcones containing amino or acetamide groups on ring A and electron donating/withdrawing groups on ring B were synthesized, and their cytotoxicity was evaluated in the present work.

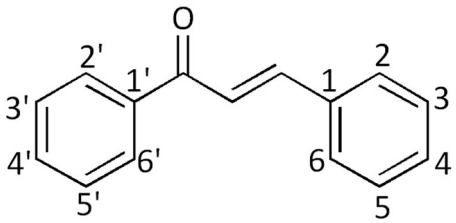

Fig. 1 Fundamental structure of a chalcone

This study describes the synthesis and characterization of twenty chalcones, including nine 4′-aminochalcones, nine 4′-acetamidechalcones, and two 3′-hydroxy-4′-methoxychalcones. Figure 2 shows the molecular structures of these twenty chalcones. Among these compounds, a new chalcone (**11**) is being reported for the first time. After the initial cytotoxic screening for all synthesized compounds, we explored the cytotoxic effect of chalcone **6a** against a panel of the tumor and nontumor cell lines. In addition, we evaluated the induction of apoptosis and cell cycle progression in HCT-116 cells incubated with chalcone **6a** for 24 h.

Materials and methods

Synthesis of the chalcones

The description of the procedure of the synthesis of the twenty chalcones are shown in Fig. 3. The 4′-aminochalcones **(1–9)** and 3′-methoxy-4′-hydroxy chalcones **(10, 11)** were synthesized by a Claisen–Schmidt condensation reaction in basic medium (Bhat et al. 2005). An ethanol solution of 4-aminoacetophenone (2 mmol) and 3-methoxy-4-hydroxyacetophenone (2 mmol) were added to a solution of benzaldehyde and the derivatives (2 mmol), followed by the addition of ten drops of 50% w/v aq. NaOH with stirring for 48 h. The solid that formed was filtered under reduced pressure, washed with cold water, and analyzed by TLC, giving yields of 25.65–69.85%. The 4′-acetamidechalcones **(1a–9a)** were prepared by the acetylation reaction of the 4′-aminochalcones (2 mmol) with acetic anhydride (2 mmol) in a buffered medium (5 mL) at pH = 5.0 with AcOH/AcONa (de Campos-Buzzi et al. 2007). The reaction mixture was refluxed for 1 h. The product was filtered under vacuum and washed with cold water, giving yields of 22.27–88.92%.

The structural data of the twenty chalcones which were synthesized in this work are given below.

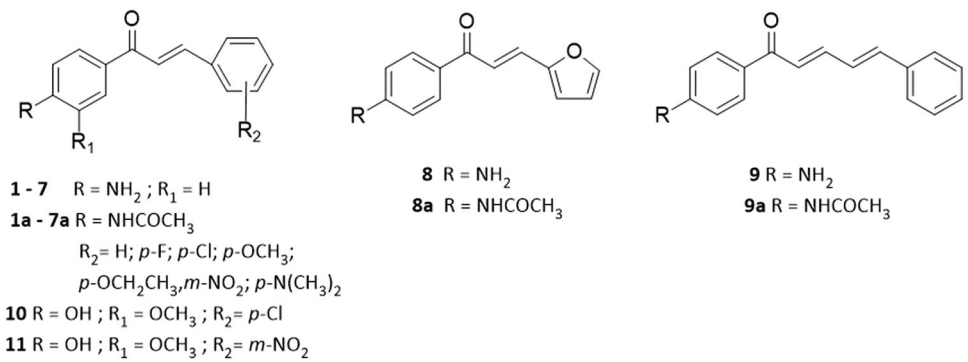

Fig. 2 Molecular structures of the synthesized chalcones

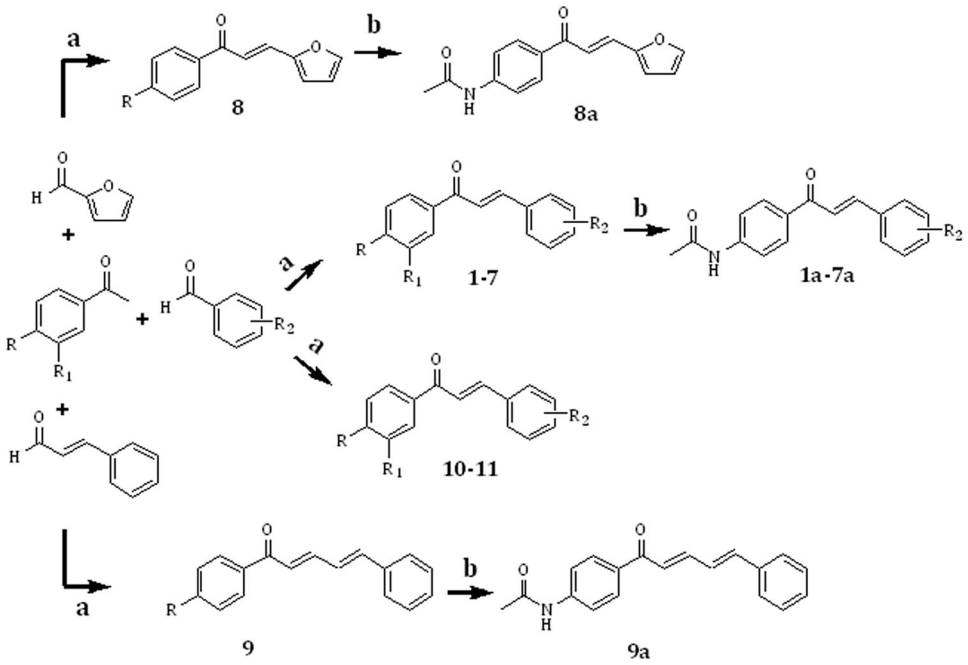

Fig. 3 Description of the procedure of the synthesis of the chalcones (**1**–**11**) and (**1a**–**9a**). **a** $NaOH_{aq}$. 50% w /v, ethanol, r. t., 48 h. **b** $(CH_3CO)_2$, (AcOH /AcONa), r.t. *Novel chalcone

Chalcone	R	R_1	R_2	Chalcone	R_2
1	NH_2	H	H	1a	H
2	NH_2	H	4-F	2a	4-F
3	NH_2	H	4-OCH_3	3a	4-OCH_3
4	NH_2	H	4-OCH_2CH_3	4a	4-OCH_2CH_3
5	NH_2	H	4-Cl	5a	4-Cl
6	NH_2	H	3-NO_2	6a	3-NO_2
7	NH_2	H	4-$N(CH_3)_2$	7a	4-$N(CH_3)_2$
8	NH_2	H		8a	
9	NH_2	H		9a	
10	OH	OCH_3	4-Cl		
11	OH	OCH_3	3-NO_2		

(2*E*)-1-(4′-aminophenyl) -3-(phenyl)-prop-2-en-1-one (1)

Yellow amorphous powder (25.65 %), m.p. 109.3–109.9 °C; FT-IR (KBr) ν_{max} 3522, 3434, 1623, 1578, 1554 cm^{-1}; ^{1}H-NMR (CD_3OD, 300 MHz): $\delta = 7.40$–7.42 (3H, m, H-3,H-5, H-4), 7.93 (2H, d, $J = 8.7$ Hz H-2′, H-6′), 6.73 (2H, d, $J =$ 8.7 Hz, H-3′, H-5′), 7.69–7.72 (4H, m, H-2/H-6, H-α, H-β). ^{13}C-NMR (CD_3OD, 75 MHz): $\delta = 136.8$ (C, C-1), 129.6 (CH, C-2, C-6), 130.1(CH, C-3, C-5), 131.4 (CH, C-4), 128.2 (C, C-1′), 132.6 (CH, C-2′, C-6′), 115.1 (CH, C-3′, C-5′), 154.8 (C, C-4′), 123.3 (CH, C-α), 144.4 (CH, C-β), 190.3 (C, COBz); EIMS *m/z* ($M^{+\cdot}$ 223), calcd for $C_{15}H_{13}NO$/223.

(2*E*)-1-(4′-aminophenyl)-3-(4-fluophenyl)-prop-2-en-1-one (2)

Yellow amorphous powder (28%), m.p. 161.5–162.5 9 °C; FT-IR (KBr) ν_{max} 3600, 1660, 1590, 1570 cm^{-1}; ^{1}H-NMR (CD_3OD, 300 MHz): $\delta = 7.76$ (2H, dd, $J = 8.8$, 2.1 Hz, H-2, H-6), 7.14 (2H, *t*, $J = 8$,8 Hz, H-3, H-5), 7.91 (2H, d, $J =$ 6.93 Hz H-2′,H-6′), 6.73 (2H, d, $J = 8.8$. Hz, H-3′, H-5′), 7.67 (1H, d, $J = 12.1$ Hz, H-α), 7.74 (1H, d, $J = 14.2$ Hz, H-β). ^{13}C-NMR (CD_3OD, 75 MHz): $\delta = 132.6$ (C, C-1), 132.6 (CH, C-2, C-6), 116.1 (CH, C-3,C-5), 163.8 (C, C-4), 128.1 (C, C-1′), 131.8 (CH, C-2′, C-6′), 114.9 (CH, C-3′,C-5′), 155.0 (C, C-4′), 123.2 (CH, C-α), 142.9 (CH, C-β), 190.1 (C, COBz); EIMS *m/z* ($M^{+\cdot}$ 241), calcd for $C_{15}H_{12}NOF$/241.

(2*E*)-1-(4′-aminophenyl)-3-(4-methoxyphenyl)-prop-2-en-1-one (3)

Yellow amorphous powder (38%), m.p.148–148,5°C; FT-IR (KBr) ν_{max} 1628, 1570, 1560 1555, 1480, 1240 cm^{-1}; ^{1}H-NMR ($CDCl_3$, 300 MHz): $\delta = 7.92$ (2H, d, $J = 8.61$ Hz, H-2,H-6), 6.70 (2H, d, $J = 8.58$ Hz, H-3,H-5), 7.59 (2H, d, $J = 8.64$ Hz, H-2′,H-6′), 6.93 (2H, d, $J = 8.67$ Hz,H-3′,H-5′), 7.42 (1H, d, $J = 15.57$ Hz, H-α), 7,76 (1H, d, $J =$

15.39 Hz, H-β), 3.89 (3H, s, OCH_3). ^{13}C-NMR ($CDCl_3$, 75 MHz): $\delta = 128.3$ (C, C-1), 131.1(CH, C-2,C-6), 114.2 (CH, C-3,C-5), 161.5 (C, C-4), 127.8 (C, C-1′), 130.2 (CH, C-2′,C-6′), 114.5 (CH, C-3′,C-5′), 151.1 (C, C-4′), 120.1 (CH, C-α), 143.2 (CH, C-β), 188.4 (C, COBz), 55.8 (CH_3, OCH_3); EIMS *m/z* ($M^{+\cdot}$ 253), calcd for $C_{16}H_{15}NO_2$/253.

(2*E*)-1-(4′-aminophenyl)-3-(4-ethoxyphenyl)-prop-2-en-1-one (4)

Yellow amorphous powder (33.89%), m.p. 140–140,8 °C; FT-IR (KBr) ν_{max} 1634, 1600, 1588, 1575, 1480, 1167 cm^{-1}; ^{1}H-NMR (CD_3OD, 300 MHz): $\delta = 7.90$ (2H, d, $J =$ 8.70 Hz, H-2,H-6), 6.69 (2H, d, $J = 8.73$ Hz, H-3,H-5), 7.63 (2H, d, $J = 7.98$ Hz, H-2′,H-6′), 6.94 (2H, d, $J = 8.70$ Hz, H-3′,H-5′), 7.58 (1H, d, $J = 15.57$ Hz, H-α), 7.65 (1H, d, $J = 15.06$ Hz, H-β), 4,08 (2H, q, $J = 6.96$, OCH_2CH_3), 1.39 (3H, *t*, $J = 6.99$ Hz, OCH_2CH_3). ^{13}C-NMR (CD_3OD, 75 MHz): $\delta = 129.3$ (C, C-1), 132.5 (CH, C-2, C-6), 114.6 (CH, C-3, C-5), 155.5 (C, C-4), 127.9 (C, C-1′), 131.4 (CH, C-2′,C-6′), 116.1 (CH, C-3′,C-5′), 162.6 (C, C-4′), 120.7 (CH, C-α), 144.4 (CH, C-β), 199.3 (C, COBz), 64.8 (CH_2, OCH_2CH_3), 15.2 (CH_3, OCH_2CH_3); EIMS *m/z* ($M^{+\cdot}$ 267), calcd for: $C_{17}H_{17}NO_2$/267.

(2E)-1-(4′-aminophenyl)-3-(4-clorophenyl)-prop-2-en-1-one (5)

Yellow amorphous powder (53.59%), m.p. 162,9–163,3 °C; FT-IR (KBr) ν_{max} 3555, 3350, 1621, 1570, 1550, 1490 cm^{-1}; ^{1}H-NMR (CD_3OD, 300 MHz): $\delta = 7.91$ (2H, d, $J = 8.73$ Hz, H-2,H-6), 7.69 (2H, d, $J = 8.79$, H-3,H-5), 7.42 (2H, d, $J = 8.46$ Hz, H-2′,H-6′), 6.68 (2H, d, $J =$ 8.76 Hz, H-3′, H-5′), 7.70 (1H, d, $J = 14.28$ Hz, H-α), 7.74 (1H, d, $J = 15.60$ Hz, H-β). ^{13}C-NMR (CD_3OD, 75 MHz): $\delta = 135.6$ (C, C-1), 132.7 (CH, C-2, C-6), 130.9 (CH, C-3, C-5), 137.5 (C, C-4), 127.6 (C, C-1′), 130.8 (CH, C-2′′,C-6′′), 114.6 (CH, C-3′,C-5′), 155.8 (C, C-4′), 124.3 (CH, C-α), 142.9 (CH, C-β), 189.9 (C, COBz); EIMS *m/z* ($M^{+\cdot}$ 257.5), calcd for: $C_{15}H_{12}NOCl$/257.5.

(2*E*)-1-(4′-aminophenyl) -3- (3-nitrophenyl) prop-2-en-1-one (6)

Orange amorphous powder (69.85%), m.p. 208–208,7 °C; FT-IR (KBr) ν_{max} 3400, 1640, 1600, 980 cm^{-1}; ^{1}H-NMR (CD_3COCD_3, 300 MHz): $\delta = 8.26$ (1H, d, $J = 1.95$ Hz, H-2), 7.98–8.26 (2H, m, H-4,H-5), 7.75 (2H, d, $J = 7.89$ Hz, H-2′,H-6′), 6.74 (2H, d, $J = 8.67$ Hz, H-3′,H-5′), 7.72 (1H, d, $J = 15.96$ Hz, H-α)), 7.80 (1H, d, $J = 17.34$ Hz, H-β). ^{13}C-NMR (CD_3COCD_3, 75 MHz): $\delta = 138.6$ (C, C-1), 124.9 (CH, C-2), 149.9 (C, C-3), 126.3 (CH, C-4), 132.2 (CH, C-5), 135.2 (CH, C-6), 127.6 (C, C-1′), 132.3 (CH, C-2′, C-6′), 114.2 (CH, C-3′,C-5′), 154.7 (C, C-4′), 123.9 (CH, C-α), 140.0 (CH, C-β), 186.9 (C, COBz); EIMS *m/z* ($M^{+\cdot}$ 268), calcd for $C_{15}H_{12}N_2O_3$/268.

(2*E*)-1-(4′-aminophenyl) -3-(4-dimethyaminophenyl) -prop-2-en-1-one (7)

Orange amorphous powder (35.66%), m.p. 169–170 °C; FT-IR (KBr) ν_{max} 3500, 3460, 1610, 1570, 1350, 1160, 980 cm^{-1}; ^{1}H-NMR (CD_3OD, 300 MHz): $\delta = 7.57$ (2H, d, $J = 8.85$ Hz, H-2, H-6), 6.69 (2H, d, $J = 8.76$ Hz, H-3,H-5), 7.89 (2H, d, $J = 8.73$ Hz, H-2′,H-6′), 6.76 (2H, d, $J =$ 8.88 Hz, H-3′,H-5′), 7.46 (1H, d, $J = 15.39$ Hz, H-α), 7.68 (1H, d, $J = 15.39$ Hz, H-β)), 3.02 (6H, s, $2CH_3$). ^{13}C-NMR (CD_3OD, 75 MHz): $\delta = 124.7$ (C, C-1), 131.5 (CH, C-2, C-6), 113.3 (CH, C-3, C-5), 153.8 (C, C-4), 40.4 (C, $N(CH_3)_2$), 128.4 (C, C-1′), 132.3 (CH, C-2′, C-6′), 114.6 (CH, C-3′,C-5′), 155.2 (C, C-4′), 117.6 (CH, C-α), 145.8 (CH, C-β), 190.8 (C, COBz); EIMS *m/z* ($M^{+\cdot}$ 266), calcd for $C_{17}H_{18}N_2O$/266.

(2*E*)-1-(4′-aminophenyl) -3- (furan-2-yl-prop-2-en-1-one (8)

Orange amorphous powder (69.85%), m.p. 118–118,3 °C; FT-IR (KBr) ν_{max} 3447, 3434, 1640, 1584, 1545, 1173 cm^{-1}; ^{1}H-NMR (CD_3OD, 300 MHz): $\delta = 6.78$ (1H, d, $J = 3.36$ Hz, H-3), 6.55 (1H, m, H-4); 7.62 (1H, s, H-5), 7,85 (2H, d, $J = 8.73$ Hz, H-2′, H-6′), 6.68 (2H, d, $J =$ 8.73 Hz, H-3′,H-5′), 7.50–7.62 (2H, s broad, H-α, H-β). ^{13}C-NMR (CD_3OD, 75 MHz): $\delta = 153.4$ (C, C-2), 113.7 (CH, C-3), 116.5 (CH, C-4), 146.3 (CH, C-5), 127.6 (C, C-1′), 132.4 (CH, C-2′, C-6′), 114.6 (CH, C-3′,C-5′), 155.5 (C, C-4′), 130.5 (CH, C-α), 120.5 (CH, C-β), 189.7 (C, COBz); EIMS *m/z* ($M^{+\cdot}$ 213), calcd for $C_{13}H_{11}NO_2$/213.

(2*E*,4*E*)-1-(4-aminophenyl)-5-phenylpenta-2,4-dien-1-one (9)

Orange amorphous powder (34.00%), m.p. 151,8–152 °C; FT-IR (KBr) ν_{max} 3458, 3376, 1635, 1611, 1576 1564 cm^{-1} ^{1}H-NMR (CD_3OD, 300 MHz): $\delta = 7.26$–7.35 (5H, m, Ar), 7.84 (2H, d, $J = 8.79$ Hz, H-2′,H-6′), 6.67 (2H, d, $J =$ 8.76 Hz, H-3′,H-5′), 7.00–7.25 (3H, m, H-α, H-7, H-8), 7.38 (1H, ddd, $J = 15.96$, 8.43, 1.65 Hz, H-β). ^{13}C-NMR (CD_3OD, 75 MHz): $\delta = 138.0$ (C, C-1), 128.7 (CH, C-2, C-6), 130.0 (CH, C-3, C-5), 128.4 (C, C-4), 126.8 (CH, C-7), 142.6 (CH, C-8), 127.7 (C, C-1′), 132.5 (CH, C-2′,C-6′), 114.6 (CH, C-3′,C-5′), 155.6 (C, C-4′), 130.5 (CH, C-α), 144.6 (CH, C-β), 190.3 (C, COBz); EIMS *m/z* ($M^{+\cdot}$ 253), calcd for $C_{17}H_{15}NO$/253.

N-(4′[(2*E*)-3-(phenyl)-1-(phenyl) prop-2-en-1-one]) acetamide (1a)

Yellow amorphous powder (88.92%), m.p. 158–158.5 °C; FT-IR (KBr) ν_{max} 3330, 1658, 1600, 1310, 980 cm^{-1}; ^{1}H-NMR (CD_3OD, 300 MHz): $\delta = 7.40$–7,72 (5H, m, Ar), 8.06 (2H, d, $J = 8.79$ Hz, H-2′, H-6′), 7.71–7.75 (2H, s broad, H-α, H-β), 2.14 (3H, s, $COCH_3$). ^{13}C-NMR (CD_3OD, 75 MHz): $\delta = 136.5$ (C, C-1), 129.8 (CH, C-2, C-6), 131.8 (CH, C-3, C-5), 131.1 (C, C-4), 134.6 (C, C-1′), 130.2 (CH, C-2′,C-6′), 123.0 (CH, C-3′,C-5′), 144.9 (C, C-4′), 24.2 (CH_3, $COCH_3$), 120.4 (CH, C-α), 145.9 (CH, C-β), 191.0 (C, COBz), 172.1 (C, N–C=O); EIMS *m/z* ($M^{+\cdot}$ 265), calcd for $C_{17}H_{15}NO_2$ /265.

N-(4′[(2*E*)-3-(4-flurophenyl) -1-(phenyl) prop-2-en-1-one]) acetamide (2a)

Yellow amorphous powder (88.21%), m.p. 178.4–179 °C; FT-IR (KBr) ν_{max} 3430, 1650, 1615, 1500, 1300, 980 cm^{-1}; ^{1}H-NMR (CD_3OD, 300 MHz): $\delta = 7.76$ (2H, m, H-2,H-6), 7.16 (2H, t, $J = 8.70$ Hz, H-3,H-5)), 8.07 (2H, d, $J =$ 8.67 Hz, H-2',H-6'), 7.73 (2H, m, H-3′,H-5′), 7,72–7.81 (2H, s broad, H-α, H-β), 2.16 (3H, s, $COCH_3$). ^{13}C-NMR (CD_3OD, 75 MHz): $\delta = 133.1$ (C, C-1), 131.1 (CH, C-2, C-6), 116.9 (CH, C-3, C-5), 164.0 (C, C-4), 132.1 (C, C-1′), 131.1 (CH, C-2′,C-6′), 122.9 (CH, C-3′,C-5′), 144.9 (C, C-4′), 120.4 (CH, C-α), 144.5 (CH, C-β), 190.8 (C, COBz), 172.1 (C, N–C=O); EIMS *m/z* ($M^{+\cdot}$ 283), calcd for $C_{17}H_{14}NO_2F$/283.

N-(4′[(2*E*)-3-(4-methoxyphenyl) -1-(phenyl) prop-2-en-1-one]) acetamide (3a)

Yellow amorphous powder (49.40%), m.p. 202.5–202.8 °C; FT-IR (KBr) ν_{max} 3260, 1640, 1600, 1310, 1160, 970 cm^{-1}; ^{1}H-NMR (CD_3OD, 300 MHz): $\delta = 7.71$ (2H, m, H-2,H-6), 7.00 (2H, d, $J = 8.70$ Hz,H-3,H-5), 8.00 (2H, d, $J =$ 8.70 Hz, H-2′,H-6′)), 7.74 (2H, d, $J = 8.55$ Hz, H-3′,H-5′), 7,72 (1H, d, $J = 15.63$ Hz, H-α), 7.76 (1H, d, $J = 16.47$ Hz, H-β), 3.85 (3H, s, OCH_3), 2.16 (3H, s, $COCH_3$). ^{13}C-NMR (CD_3OD, 75 MHz): $\delta = 129.1$ (C, C-1), 131.4 (CH, C-2, C-6), 115.7 (CH, C-3,C-5), 163.6 (C, C-4), 132.6 (C, C-1′), 131.8 (CH, C-2′,C-6′), 120.4 (CH, C-3′,C-5′), 146.2 (C, C-4′), 120.4 (CH, C-α), 144.7 (CH, C-β), 191.1 (C, COBz), 172.1 (C, N–C=O), 56.1 (C, OCH_3); EIMS *m/z* ($M^{+\cdot}$ 295), calcd for $C_{18}H_{17}NO_3$/295.

N- (4′- [(2*E*) -3- (4-ethoxyphenyl) -1- (phenyl) prop-2-en-1-one]) acetamide (4a)

Yellow amorphous powder (38.02%), m.p. 134–135 °C; FT-IR (KBr) ν_{max} 3310, 1650, 1670, 1600, 1310, 1155, 980 cm^{-1}; ^{1}H-NMR ($CDCl_3$, 300 MHz): $\delta = 7.57$ (2H, d, $J = 8.50$ Hz, H-2,H-6), 6.91 (2H, d, $J = 8.45$ Hz, H-3,H-5), 8.00 (2H, d, $J = 8.40$, H-2′H-6′), 7.66 (2H, d, $J = 7.75$ Hz, H-3′,H-5′), 7.39 (1H, d, $J = 15.55$ Hz, H-α), 7.78 (1H, d, $J = 15.60$ Hz, H-β), 4.08 (2H, q, $J = 6.85$ Hz, OCH_2CH_3), 1.43 (3H, t, $J = 6.90$ Hz, OCH_2CH_3), 2.21 (3H, s, $COCH_3$). ^{13}C-NMR ($CDCl_3$, 75 MHz): $\delta = 127.6$ (C, C-1), 130.0 (CH, C-2, C-6), 115.1 (CH, C-3, C-5), 161.3 (C, C-4), 134.2 (C, C-1′), 130.5 (CH, C-2′, 6′), 119.2 (CH, C-3′,5′), 142.3 (C, C-4′), 63.9 (CH_2, OCH_2CH_3), 14.9 (CH_3, OCH_2CH_3), 25.0 (CH_3, $COCH_3$), 119.5 (CH, C-α), 144.8 (CH, C-β), 189.4 (C, COBz), 168.9 (C, N–C=O); EIMS *m/z* ($M^{+\cdot}$ 309), calcd for $C_{19}H_{19}NO_3$/309.

N-(4′[(2*E*)-3-(4-clorophenyl-1-(phenyl) prop-2-en-1-one]) acetamide (5a)

Yellow amorphous powder (54.02%), m.p. 198.5–199 °C; FT-IR (KBr) ν_{max} 3270, 1650, 1600, 1310, 980 cm^{-1}; ^{1}H-NMR (CD_3OD, 300 MHz): $\delta = 7.42$ (2H, d, $J = 8.49$ Hz, H-2,H-6), 7.90 (2H, d, $J = 8.76$ Hz, H-3,H-5), 8.00 (2H, d, $J = 8.79$ Hz, H-2′,H-6′), 6,69 (2H, d, $J = 8$,76 Hz, H-3′,H-5′), 7.40 (1H, d, $J = 17.04$ Hz, H-α,), 8.71 (1H, d, $J =$ 14.88 Hz, H-β), 2.15 (3H, s, $COCH_3$). ^{13}C-NMR (CD_3OD, 75 MHz): $\delta = 134.5$ (C, C-1), 130.4 (CH, C-2, C-6), 131.0 (CH, C-3, C-5), 137.5 (C, C-4), 135.3 (C, C-1′), 132.7 (CH, C-2′,6′), 120.4 (CH, C-3′5′), 142.6 (C, C-4′), 130.3 (CH, C-α), 145.0 (CH, C-β), 190.0 (C, COBz), 172.1 (C, N–C=O), 24.2 (CH_3, COCH3); EIMS *m/z* ($M^{+\cdot}$ 283.5), calcd for $C_{17}H_{14}NOCl$/283.5.

N- (4′- [(2*E*) -3- (3-nitrophenyl) -1- (phenyl) prop-2-en-1-one]) acetamide (6a)

Orange amorphous powder (51.29%), m.p. 198–198,3 °C; FT-IR (KBr), ν_{max} 3330, 1610, 1660, 1580, 1340, 970 cm^{-1}; ^{1}H-NMR (CD_3SOCD_3, 300 MHz): $\delta = 8.17$–7.75 (2H, m, H-4, H-5), 8,17 (1H, d, $J = 10.53$ Hz, H-6), 7.96 (2H, d, $J = 7.41$ Hz, H-2′,H-6′), 6.63 (2H, d, $J = 7.32$ Hz, H-3′,H-5′), 8.00 (1H, d, $J = 17.04$, H-α), 8.71 (1H, d, 14.88 Hz, H-β), 2.09 (3H, s, $COCH_3$). NMR de ^{13}C (CD_3SOCD_3, 75 MHz): $\delta = 134.9$ (C, C-1), 122.8 (CH, C-2), 148.4 (C, C-3), 122.6 (CH, C-4), 130.1 (C, C-5), 134.7 (CH, C-6), 137.1 (C, C-1′), 131.4 (CH, C-2′, C-6′), 112.9 (CH, C-3′,5′), 144.0 (C, C-4′), 122.9 (CH, C-α), 144.0 (C, C-β), 187.4 (C, COBz), 169.2 (C, N–C=O), 24.2 (CH_3, $COCH_3$); HRESIMS, *m/z*: 310.1445($C_{19}H_{19}NO_3$) $[M+H]^+$ (calcd. 310.1443).

N-(4′[(2*E*)-3-(4-dimetilaminophenyl) -1-(phenyl) prop-2-en-1-one]) acetamide (7a)

Yellow amorphous powder (60.40%), m.p. 207–207.5 °C; FT-IR (KBr) ν_{max} 3410, 1680, 1650, 1580, 1380, 1030 cm

$^{-1}$; ^{1}H-NMR ($CDCl_3$, 300 MHz): $\delta = 7.66$ (2H, d, $J =$ 8,20 Hz, H-2,H-6)), 7.53 (2H, d, $J = 8.65$ Hz H-3,H-5), 8.00 (2H, d, $J = 8.30$ Hz, H-2′,H-6′), 6.71 (2H, d broad, H-3′/H-5′), 7.34 (1H, d, $J = 15.45$ Hz, H-α), 7.78 (1H, d, $J =$ 15.45 Hz, H-β), 3.04 (6H, s, $2CH_3$), 2.21 (3H, s, $COCH_3$). ^{13}C-NMR ($CDCl_3$, 75 MHz): $\delta = 134.6$ (C, C-1), 130.1 (CH, C-2, C-6), 112.3 (CH, C-3,C-5), 152.0 (C, C-4), 40.5 (C, $N(CH_3)_2$), 133.0 (C, C-1′), 130.6 (CH, C-2′,C-6′), 116.9 (CH, C-3′,C-5′), 145.7 (C, C-4′), 24.9 (CH_3, $COCH_3$), 119.2 (CH, C-α), 142.0 (CH, C-β), 189.5 (C, COBz), 169.0 (C, N–C=O), 40.5(C, $N(CH_3)_2$), 24.9(CH_3, $COCH_3$); EIMS *m/z* ($M^{+\cdot}$ 308), calcd for $C_{19}H_{20}N_2O_2$/308.

N-(4′[(2*E*)-3- (furan-2-il) -1-(phenyl) prop-2-en-1-one]) acetamide (8a)

Orange amorphous powder (76.17%), m.p. 122–122.4 °C; FT-IR (KBr) ν_{max} 3470, 1690, 1640, 1600, 1375, 1005 cm $^{-1}$; ^{1}H-NMR ($CDCl_3$, 300 MHz): $\delta = 6.51$ (1H, s broad, H-3), 6.70 (1H, d, $J = 3{,}09$ Hz, H-4), 7.46 (1H, s, H-5), 8.00 (2H, d, $J = 8{,}55$ Hz, H-2′, H-6′), 7.66 (2H, d, $J = 8{,}31$ Hz, H-3′, H-5′), 7.33 (1H, d, $J = 15.33$ Hz, H-α), 7.51 (1H, d, $J = 17.58$ Hz, H-β), 2.21 (3H, s, $COCH_3$). ^{13}C-NMR ($CDCl_3$, 75 MHz): $\delta = 151.9$ (C, C-2), 112.7 (CH, C-3), 116.2 (CH, C-4), 145.1 (CH, C-5), 133.9 (C, C-1′), 130.0 (CH, C-2′, C-6′), 119.3 (CH, C-3′, C-5′), 24.8 (CH_3, $COCH_3$), 119.4 (CH, C-α), 130.7 (CH, C-β), 188.8 (C, COBz), 169.0 (C, N–C=O), 24.9 (CH_3, $COCH_3$); EIMS *m/z* ($M^{+\cdot}$ 239), calcd for $C_{15}H_{13}NO_2$/239.

N-(4′[(2*E*)-5-[phenylpenta-2,4-dien) -1-(phenyl) prop-2-en-1-one]) acetamide (9a)

Orange amorphous powder (22.27%), m.p. 176.5–177 °C; FT-IR (KBr) ν_{max} 3300, 1670, 1650, 1600, 1300, 1000 cm^{-1}; ^{1}H-NMR ($CDCl_3$, 300 MHz): $\delta = 7.33$–7.40 (5H, m, Ar), 7.98 (2H, d, $J = 8{,}64$ Hz, H-2′,H-6′), 7.01 (2H, d, $J = 7.71$ Hz, H-3′,H-5′), 7.19 (1H, d, $J = 14.79$ Hz, H-α), 7.51 (1H, dd, $J = 17.40$, 8.76 Hz, H-β), 7.02–7.07 (2H, m, H-7,H-8), 2.23 (3H, s, $COCH_3$). ^{13}C-NMR ($CDCl_3$, 75 MHz): $\delta = 136.4$ (C, C-1), 127.5 (CH, C-2, C-6), 129.1 (CH, C-3,C-5), 129.4 (C, C-4), 134.1 (C, C-1′), 130.0 (CH, C-2′, C-6′), 119.2 (CH, C-3′, C-5′), 142.1 (C, C-4′), 24.9 (CH_3, $COCH_3$), 127.2 (CH, C- α), 144.8 (CH, C-β), 125.4 (CH, C-7), 142.0 (CH, C-8), 189.2 (C, COBz), 168.8 (C, N–C=O), 24.9 (CH_3, $COCH_3$); EIMS *m/z* ($M^{+\cdot}$ 291), calcd for $C_{19}H_{17}NO_2$/291.

(2*E*)-1-(3′-methoxi-4′-hidroxiphenyl)-3-(4-clorophenyl)-prop-2-en-1-one (10)

Yellow amorphous powder (20.89%), m.p. 141–141.3 °C; FT-IR (KBr) ν_{max} 3390, 1640, 1590, 1290, 1180, 970 cm^{-1}; ^{1}H-NMR (CD_3COCD_3, 300 MHz): $\delta = 7.50$ (2H, d, $J =$ 7,50 Hz, H-2,H-6), 7.70 (2H, d, $J = 8.73$ Hz, H-3, H-5), 7.76 (1H, d, $J = 1.92$ Hz, H-2′), 6.70 (1H, d, $J = 8.22$ Hz, H-5′), 7.74 (1H, dd, $J = 8.85$, 2.01 Hz, H-6′), 7.73 (1H, d, $J = 17.90$ Hz, H-α), 7.91 (1H, d, $J = 15.48$ Hz, C-β), 3.90 (3H, s, OCH_3). ^{13}C-NMR (CD_3COCD_3, 75 MHz): $\delta =$ 135.3 (C, C-1), 129.9 (CH, C-2,C-6), 130.9 (CH, C-3, C-5), 136.9 (C, C-4), 136.2 (C, C-1‘), 112.6 (CH, C-2′), 148.7 (C, C-3′), 152.7 (C, C-4′), 115.6 (CH, C-5′), 124.6 (CH, C-6′), 123.7 (CH, C-α), 142.2 (CH, C-β), 56.5 (C, OCH_3), 187.9 (C, COBz); EIMS *m/z* ($M^{+\cdot}$ 288.5), calcd for $C_{16}H_{13}NO_3Cl$ /288.5.

(2*E*) -1- (3′-methoxy-4′-hydroxyphenyl) -3- (3-nitrophenyl) prop-2-en-1-one (11)

Yellow amorphous powder (46.33%), m.p. 179.4–180 °C; FT-IR (KBr) ν_{max} 3425, 1621, 1575, 1350, 990 cm^{-1}; ^{1}H-NMR (CD_3COCD_3, 300 MHz): $\delta = 6.96$–8.26 (5H, m, Ar), 8.65 (1H, s, H-2′), 7.73 (1H, m, H-5′), 8.23 (1H, d, $J =$ 6.36 Hz, H-6′), 7.82 (1H, d, $J = 15.35$ Hz, H-α), 7.87 (1H, d, $J = 15.35$ Hz, H-β), 3.90 (3H, s, OCH_3). ^{13}C-NMR (CD_3COCD_3, 75 MHz): $\delta = 131.1$ (C, C-1), 124.9 (CH, C-2), 152.9 (C, C-3), 125.1 (CH, C-4), 131.2 (CH, C-5), 135.4 (CH, C-6), 138.3 (C, C-1′), 124.9 (CH, C-2′), 148.8 (C, C-3′), 149.9 (C, C-4′), 115.6 (CH, C-5′), 125.8 (CH, C-6′), 123.5 (CH, C-α), 141.1 (CH, C-β), 56.5 (C, OCH_3), 187.8 (C, COBz); HRESIMS *m/z*: 300.0867 ($C_{16}H_{13}NO_3$) $[M+H]^+$ (calcd. 300.0872).

NMR, GC–MS, and IR measurements

The chemical reagents were from Sigma-Aldrich. ^{1}H and ^{13}C NMR spectra were obtained using a Bruker Spectrometer, either model Avance DPX-300 or model Avance DRX-500 operating at frequencies of 300 or 500 MHz for hydrogen, and 75 or 125 MHz for carbon, respectively. The spectra were measured in the solvents CD_3OD, CD_3COCD_3, and $CDCl_3$, and chemical shifts are reported as δ values in parts per million (ppm) relative to tetramethylsilane (δ 0.00) as the internal standard. The mass spectra were obtained with a Shimadzu QP201 GC-MS (gas chromatography coupled to mass spectrometry) using an RTX-5MS capillary column (30.0 m × 0.25 mm × 0.30 mm) for compounds within the literature record, and UPLC-QTOF-MS was performed with an ACQUITY UPLC BEH column (150 × 2.1 mm, 1.7 µm; Waters Co.) on a Waters Acquity UPLC system. The column temperature was set at 40 °C. The binary gradient elution system consisted of 0.1% formic acid in water (A) and 0.1 % formic acid in acetonitrile (B), with a linear gradient from 2 to 95% B (0–15 min), with a flow rate of 0.4 mL.min^{-1} for the new compound (**11**). The high mass spectra of the chalcone 11

was obtained with LC–MS on an Acquity UPLC system coupled with quadrupole/TOF mass analyzers (Waters) equipped with an ESI source operated in the negative ionization mode (UPLC-ESI-qTOF). The chromatographic separations were performed using a Waters Acquity UPLC BEH column (150.0 × 2.1 mm × 1.7 µm) at 40 °C. Water and acetonitrile were used for the mobile phase, both with 0.1% formic acid. The gradient ranged from 95 to 2% water in 15 min at a flow rate of 0.4 mL/min and an injection volume of 5.0 µL. The desolvation gas was N_2 at 350 °C at a flow rate of 350 L/h and a source temperature of 120 °C. The capillary voltage was set to 2.600 V. The collision energies/cone voltages were set to 6 eV/15 V (low) and 30–50 eV/30 V (high) to achieve sufficient fragmentation. The MS spectra were acquired in negative ionization mode between 100 and 1180 Da in MSE tandem mode. The samples were prepared by filtering 1 mL of the chalcones directly through a 0.22 µm PTFE syringe filter (Simple Pure, USA). Infrared spectra were determined on a Perkin Elmer FT/IR 1000 spectrophotometer and reported as the wavenumber (cm^{-1}). The melting point was determined with the MQAPF-302 apparatus (microchemistry) with a heating rate of 3.0 °C/min.

Cell culture

The human cancer cell lines (HCT-116, colon carcinoma; PC-3, prostate adenocarcinoma; HL-60, promyelocytic leukemia; K-562, chronic myeloid leukemia; and KASUMI-1, acute myeloid leukemia) were obtained from the National Cancer Institute, Bethesda, MD, USA. The L-929 (murine fibroblasts) nontumor cell line was purchased from ATCC® and deposited in the Rio de Janeiro cell bank. The cell lines were maintained in RPMI-1640 medium or DMEM (Gibco) supplemented with 10% fetal bovine serum, 2 mM glutamine, 100 U/mL penicillin, and 100 µg/mL streptomycin at 37 °C in a humidified atmosphere with 5% CO_2.

Determination of cytotoxic activity

The cytotoxicity of the compounds was determined using the MTT assay (Mosmann 1983). Briefly, cells were seeded in 96-well plates (0.7×10^4 cells/well for adherent cells and 0.3×10^5 cells/well for suspended cells). The compounds dissolved in DMSO were added to each well using high-throughput screening with a Biomek 3000 (Beckman Coulter, Inc. Fullerton, California, USA) and incubated for 3 days (72 h). The control group received the same amount of vehicle, and the final concentration of DMSO in the culture media was constant (below 0.5%). After incubation, the supernatant was replaced by fresh medium containing MTT (0.5 $mg.mL^{-1}$). Three hours later, the MTT formazan product was dissolved in 150 µL of DMSO, and the absorbance was measured at 595 nm (DTX 880 Multimode Detector, Beckman Coulter, Inc. Fullerton, California, USA).

To carry out a structure-activity relationship analysis, all compounds were tested against HCT-116 cells at different concentrations (0.04–20 µM) to determine the half-maximal inhibitory concentration (IC_{50}) after 72 h of incubation. In addition, the IC_{50} value of the most active compound was determined for four other human tumor cell lines (PC-3, HL-60, K-562, and KASUMI-1) and one nontumor cell line (L-929) after 72 h of incubation. Doxorubicin (0.07–8.6 µM; Sigma Chemical Co. St. Louis, MO, USA) was used as a positive control.

Study of the mechanism of cytotoxicity

In this stage, the study aimed to describe the chalcone **6a**-induced cytotoxicity against HCT116 cells (chosen based on the preliminary cytotoxicity screening). For this purpose, the cells (0.7×10^5 cells/well) were incubated with the chalcone **6a** for 24 h at three different concentrations (2.5, 5 and 10 µM; chosen based on the IC_{50} values obtained by the MTT assay), and the experiments below were performed (Pereira et al. 2016). The control group received the same amount of vehicle whose concentration was kept constant (below 0.5%). Cell treatments were carried out in triplicate. Doxorubicin (2 µM; Sigma Chemical Co. St. Louis, MO, USA) was used as a positive control due to its known cytotoxic effects, as well as its ability to induce cell cycle arrest in the G2/M phase. Stock solutions of the compounds tested were prepared in DMSO and diluted in culture medium to obtain the desired concentrations.

Morphological analysis

The morphological features of HCT116 cells were assessed using light microscopy (Olympus, Tokyo, Japan). Cells were harvested, transferred to Cytospin slides, and stained using a quick panoptic kit (Laborlin, Brazil). Cells were fixed with methanol and counterstained with 0.1% xanthanes and 0.1% thiazines before the analysis.

Apoptosis assay

Apoptosis was examined by Annexin V/7-AAD staining followed by flow cytometry. Briefly, HCT116 cells were collected (both floating and attached cells) and stained using an Annexin V-PE/7-AAD apoptosis detection kit. Annexin V binds to phosphatidylserine (PS) in cells undergoing apoptosis due to the translocation of PS from the inner leaflet to the outer leaflet of the cytoplasmic membrane. 7-AAD is a fluorescent intercalator of DNA impermeant to the cell, indicating membrane integrity. Double staining is used to distinguish between viable, early apoptotic cells, and necrotic

or late apoptotic cells. The resulting fluorescence (Annexin V-PE at 583 nm and 7-AAD at 680 nm) of all samples was analyzed with BD FACSVerse™. 7-AAD-positive and annexin V-negative cells were considered necrotic. Annexin V-positive cells (both 7-AAD positive and negative cells) were considered apoptotic cells. 7-AAD-negative and Annexin V-negative cells were considered viable.

Determination of cell viability and membrane integrity

Cell viability and cell membrane integrity analyses were performed with propidium iodide (5 µg/mL, Sigma Aldrich Co., St. Louis, MO, USA) exclusion using flow cytometry. HCT116 cells were plated in 24-well plates and treated with PJOV56. After cell harvesting, the treated and untreated cells were incubated with propidium iodide in the dark for 5 min. Then, the fluorescence was measured by flow cytometry with BD FACSVerse™ (BD Biosciences, San Jose, CA).

DNA fragmentation and cell cycle analysis

The DNA content of HCT116 cells was assessed by propidium iodide DNA staining followed by flow cytometry analysis. Briefly, cells were treated with PJOV56, harvested and incubated in the dark with a solution containing 5 µg. mL^{-1} propidium iodide, 5 µg.mL^{-1} RNase, 0.1 % sodium citrate, and 0.1 % Triton X-100 at room temperature for 40 min. The DNA fragmentation and cell cycle profile were obtained by cell counting and fluorescence measurements using a BD FACSVerse™ flow cytometer (BD Biosciences, San Jose, CA). Data were analyzed by ModFit LT software (Verity Software House, Inc., Topsham, ME).

Statistical analysis

Data are presented as the mean ± standard error of the mean (SEM) from three independent experiments performed in triplicate as calculated by Prism 8.0 (GraphPad/Intuitive Software for Science, San Diego, CA). The IC_{50} values of the compounds were obtained from the nonlinear regression of the cytotoxicity curves. Statistical analyses for multiple comparisons were performed using one-way ANOVA followed by Turkey's Test. A value of $p < 0.05$ was considered statistically significant.

Results and discussion

Structural characterization

The structures of the twenty synthetic chalcones were elucidated by spectroscopic methods, including 1D NMR for those chalcones registered in the literature, and 1D and 2D (COSY, HSQC and HMBC) NMR for the new chalcone (**11**), electron ionization mass spectrometry, high-resolution electrospray ionization mass spectrometry (HRESIMS), and Fourier-transform infrared spectroscopy (FT-IR). The ^{1}H (500 MHz) and ^{13}C (125 MHz) NMR spectra in $CDCl_3$ (d, ppm, J/Hz) are presented in the Supplementary Material in Figs S1–S44. The mass spectra of these chalcones are shown in Figs S45–S64 and their infrared spectra are given in Figs S65–S84. The values of the coupling constants between H_α and H_β ($J = 12.10$–17.98 Hz) confirm that for this reaction, the products generated were only *E*-isomers.

Cytotoxic activity against tumor and nontumor cells

The MTT assay was used to determine the cytotoxicity of the synthesized chalcones. This test is extremely useful for both determining cell viability studies and defining the anticancer potential of new compounds (Kepp et al. 2011). Table 1 displays the IC_{50} values of the investigated compounds whose data were used for the structure–activity relationship analysis.

Out of 20 compounds tested, only **1a** ($IC_{50} = 4.96 \pm 0.03$ µM), **2a** ($IC_{50} = 7.05 \pm 0.02$ µM), **5a** ($IC_{50} = 5.75 \pm 0.44$ µM), and **6a** ($IC_{50} = 3.56 \pm 0.03$ µM) showed a strong cytotoxic effect ($IC_{50} < 10$ µM) against HCT-116 cells, revealing that small modifications to the chalcone chemical structure were able to alter the biological activity. Careful analysis of the structures suggests that the cytotoxicity can be attributed to the combined effects of the two electron-withdrawing groups in the structure of **6a** (an amide group on ring A and a nitro group on ring B). For the amide group contribution, compound **1a** ($IC_{50} = 4.96 \pm 0.03$ µM) presented higher cytotoxic activity when compared to **1** ($IC_{50} > 20$ µM). Regarding the nitro group, compounds **6** ($IC_{50} = 13.96 \pm 0.03$ µM) and **6a** ($IC_{50} = 3.56 \pm 0.03$ µM) presented greater activity when compared with **1** and **1a**, respectively. Moreover, the presence of an extended conjugated system significantly reduced the cytotoxic effect. Compound **9a** ($IC_{50} > 20$ µM) showed no cytotoxic effect when compared to compound **1a** ($IC_{50} = 4.96 \pm 0.03$ µM), and this effect was influenced by the presence of an additional double bond in the conjugated system. Another important structural feature that reduced the cytotoxic activity was a high electronic density in ring B ($IC_{50} > 20$ µM) for compounds **3**, **3a**, **4**, **4a**, **7** (% RCV = 4.25 ± 2.60 %), **7a** (% RCV = 0.00 %), **8** (% RCV = 9.15 ± 3.01 %), and **8a** (% RCV = 9.45 ± 1.37 %). These data are corroborated by a review of the anticancer activity of chalcones that states that the cytotoxic properties of chalcones against cancer cell lines are mainly influenced by the substituents on the two aryl rings of the chalcone molecule simultaneously (Karthikeyan et al. 2015). Recent studies (Nazir et al. 2013; Guilherme et al.

Table 1 Cytotoxicity of the chalcones **1**–**11** and **1a**–**9a** at different concentrations (0.02–20 μM) against HCT-116 cells (human colon carcinoma) after 72 h of incubation using MTT assay

Chalcone	Chemical group[b]			HCT-116
	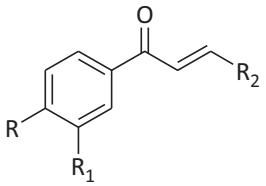			
	R	R_1	R_2	IC_{50} ± S.E.M. (μM)[a]
1	NH_2	H	Ph	>20
1a	–$NHCOCH_3$	H	Ph	4.96 ± 0.03
2	NH_2	H	*p*-F-Ph	15.16 ± 0.06
2a	–$NHCOCH_3$	H	*p*-F-Ph	7.05 ± 0.02
3	NH_2	H	*p*-OCH_3-Ph	>20
3a	–$NHCOCH_3$	H	*p*-OCH_3-Ph	>20
4	NH_2	H	*p*-OCH_2CH3-Ph	>20
4a	–$NHCOCH_3$	H	*p*-OCH_2CH3-Ph	>20
5	NH_2	H	*p*-Cl-Ph	>20
5a	–$NHCOCH_3$	H	*p*-Cl-Ph	5.75 ± 0.44
6	NH_2	H	*m*-NO_2-Ph	13.96 ± 0.03
6a	–$NHCOCH_3$	H	*m*-NO_2-Ph	3.56 ± 0.03
7	NH_2	H	*p*-$N(CH_3)_2$-Ph	>20
7a	–$NHCOCH_3$	H	*p*-$N(CH_3)_2$-Ph	>20
8	NH_2	H	Furan-2-il	>20
8a	–$NHCOCH_3$	H	Furan-2-il	>20
9	NH_2	H	Phenylpenta-4-en	>20
9a	–$NHCOCH_3$	H	Phenylpenta-4-en	>20
10	OH	OCH_3	*p*-Cl-Ph	>20
11	OH	OCH_3	*m*-NO_2-Ph	>20

[a]Data are presented as half maximal inhibitory concentration (IC_{50} in μM) ± Standard Error of the Mean (S.E.M.) obtained from three independent experiments performed in triplicate

[b]Specific chemical groups of each compound bonded to fundamental core

2015) have also demonstrated the high cytotoxic effects of nitro- and amide-containing chalcones against various types of human cancer cell lines, including colon cancer. Moreover, Guo et al. (2018) showed that a synthetic compound bearing the strongly electron-withdrawing NO_2 group displayed the highest anticancer activity (7.3 ± 1.2 μM) against the A549 cell line (lung cancer) compared with the other synthesized compounds. All of these findings reinforce the synthetic proposal of the present work. For these reasons, chalcone **6a** was selected for further IC_{50} value determination against four human tumor cell lines (PC-3, HL-60, K-562, and KASUMI-1) and nontumor murine fibroblasts (L-929 cells). Table 2 shows the cytotoxicity of chalcone 6a at different concentrations (0.02–20 μM) against six cell lines after 72 h of incubation using MTT assay. Against the tumor cells, the IC_{50} values of **6a** ranged from 5.65 to 10.52 μM (strong cytotoxic activity). Against L-929 cells, compound **6a** was not active (IC_{50} > 20 μM). This suggests that there are specific characteristics of the tumor cells that are being affected by compound **6a** at the tested concentrations. In fact, cancer has six biological capabilities, including sustaining proliferative signaling, evading growth suppressors, resisting cell death, enabling replicative immortality, inducing angiogenesis, and activating invasion and metastasis (Hanahan and Weinberg 2011). In this context, Karthikeyan et al. (2015) reported the cytotoxic activity of chalcones through multiple mechanisms, including cell cycle disruption, angiogenesis inhibition, tubulin polymerization inhibition, apoptosis induction, blockade of the NF-κB signaling pathway, and inhibition of cell cycle regulatory kinases.

Mechanism of cytotoxicity against human colon cancer cells

Based on the initial data indicating the in vitro cytotoxic potential of the chalcone **6a**, we decided to investigate the pattern of cell death induced by this chalcone in HCT-116 cells at three concentrations (2.5, 5, and 10 μM) after 24 h of incubation. First, microscopic analysis showed that

Table 2 Cytotoxicity of chalcone **6a** at different concentrations (0.02–20 μM) against six cell lines after 72 h of incubation using MTT assay

Chalcone	Cell line					
	HCT-116	PC-3	HL-60	K-562	KASUMI-1	L-929
	IC_{50} ± S.E.M. (μM)[a]					
6a	3.56 ± 0.03	9.33 ± 0.05	5.65 ± 0.41	7.49 ± 1.35	10.52 ± 0.10	>20
Dox[b]	0.11 ± 0.03	0.44 ± 0.10	0.02 ± 0.002	0.46 ± 0.01	0.13 ± 0.007	0.66 ± 0.17

[a]Data are presented as half maximal inhibitory concentration (IC_{50} in μM) ± Standard Error of the Mean (S.E.M.) for tumor cells (HCT-116, human colon carcinoma; PC-3, human prostate adenocarcinoma; HL-60, human promyelocytic leukemia; K-562, human chronic myeloid leukemia; and KASUMI-1, human acute myeloid leukemia), and nontumor cells (L-929, murine fibroblast), obtained from at least two independent experiments performed in triplicate

[b]Doxorubicin (**Dox**, 0.07–8.6 μM) was used as positive control of the assay

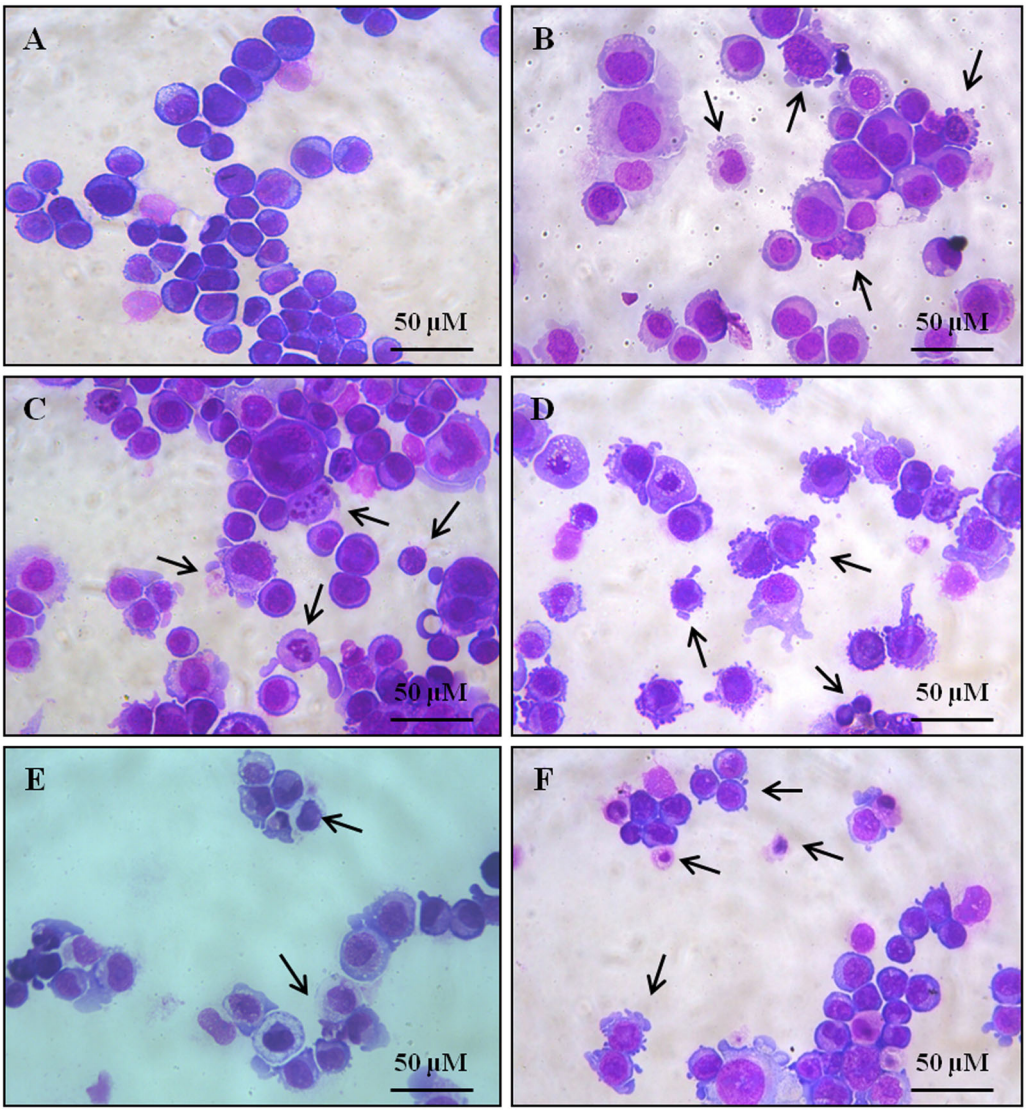

Fig. 4 Effect of chalcone **6a** on the morphology of HCT-116 cells determined by light microscopy (400×) using panoptic kit after 24 h of incubation. Cells untreated (**a**) or treated with chalcone **6a** (2.5 µM, **c**; 5 µM, **d**; and 10 µM, **e**) were fixed with methanol and counter-stained with 0.1% xanthanes and 0.1% thiazines before the analysis. Black arrows show apoptotic cells (nuclear fragmentation, chromatin condensation, apoptotic bodies, and cell shrinkage)

chalcone **6a** was able to induce morphological changes in HCT-116 cells that were characteristic of apoptosis (nuclear fragmentation, chromatin condensation, apoptotic bodies, and cell shrinkage), and these changes were more evident at the concentrations of 5 and 10 µM (Fig. 4d, e) (Kroemer et al. 2008).

Chalcone **6a-**induced apoptosis was confirmed by the externalization of phosphatidylserine accompanied by maintenance of membrane integrity and a reduction in the number of cells as determined by flow cytometry (Figs 5 and 6). At 10 µM, chalcone **6a** induced a significant increase in apoptotic cells (9.60 ± 1.68 %) when compared with the negative control (1.55 ± 0.18 %). At this concentration, we also observed 90.29 ± 0.62 % membrane integrity (no difference when compared with the negative control value of 95.10 ± 0.55 %) and $4.21 \pm 0.19 \times 10^5$ cells/mL (statistically significant when compared with the negative control, $7.34 \pm 0.35 \times 10^5$ cells/mL) after 24 h of incubation. Corroborating these results, Das and Manna (2016) highlighted the participation of apoptosis in the anticancer activity of chalcones. Specifically, against human colon cancer, apoptosis induction might be correlated with a cell cycle arrest in the G2/M phase, involving disruption of the microtubular network and/or DNA damage. The mitotic spindle network is critical for the process of cell division, whereas disruption leads to apoptosis (Bond et al. 2018).

In this work, we confirmed this effect for chalcone **6a** against HCT-116 cells (Fig. 7). Similar to the positive control

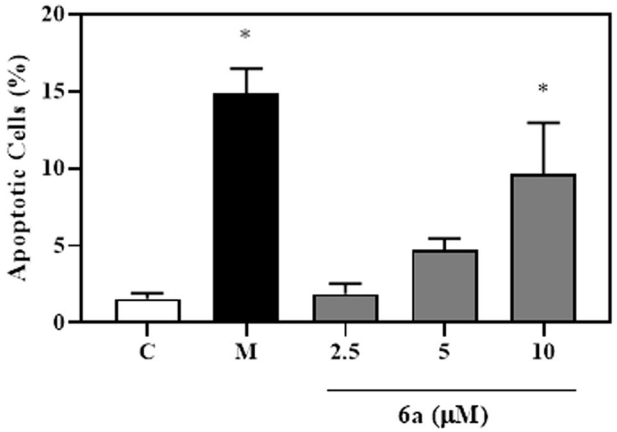

Fig. 5 Effect of chalcone **6a** on the PS externalization of HCT-116 cells determined by flow cytometry using Annexin V-PE/7-AAD after 24 h of incubation. Data are presented as mean ± S.E.M. from three independent experiments performed in triplicate. *$p < 0.05$ compared with negative control (**c**) by One-way ANOVA followed by the Turkey's Test. Ten thousand events were analyzed in each experiment, and menadione (M; 20 μM) was used as positive control

doxorubicin (2 μM; %G2/M = 79.78 ± 1.35 %), chalcone **6a** induced significant G2/M arrest (59.87 ± 5.15 %) in HCT-116 cells when compared with the negative control (treated with only vehicle; %G2/M = 36.70 ± 2.47 %). This means that compound **6a** may interfere with the process of cellular division that is detectable by cell cycle checkpoints (Das and Manna 2016). Consequently, the cells are triggered to cell death by apoptosis, as we can observe in the data shown above (morphological and flow cytometry data). It is worth mentioning that the chalcone **6a** was not able to induce DNA at the tested concentrations and incubation time (data not shown). It seems that DNA fragmentation is not involved with the chalcone **6a**-induced cell cycle arrest in HCT-116 cells, at least not as a starting point. This evidence reinforces the hypothesis of mitotic spindle network interference that shall be investigated further. In fact, Martel-Frachet et al. (2015) identified a new chalcone derivative that is capable of inducing prometaphase arrest and subsequent apoptosis of bladder cancer cells that acts as a microtubule inhibitor. Finally, it is important to note that additional tests are necessary to evaluate the specific mechanism of action involved in the selective cytotoxicity of chalcone **6a** against HCT-116 cells.

Conclusions

A series of twenty *E*-isomer chalcones were synthetized by the Claisen–Schmidt condensation reaction; nine 4′-aminochalcones, nine 4′-acetamidechalcones, and two 3′-methoxy-4′-hydroxychalcones. Regarding cytotoxic activity, this work demonstrated that small changes in the

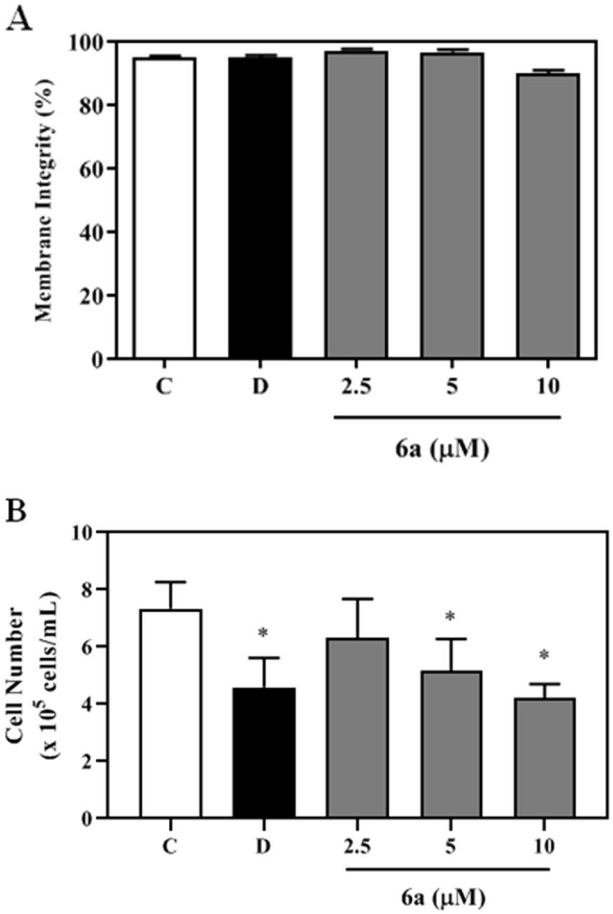

Fig. 6 Effect of chalcone **6a** on cell membrane integrity (**a**) and cell number (**b**) of HCT-116 cells determined by flow cytometry using propidium iodate (PI) after 24 h incubation. Data are presented as mean ± S.E.M. from three independent experiments performed in triplicate. *$p < 0.05$ compared with negative control (**c**) by One-way ANOVA followed by the Turkey's Test. Ten thousand events were analyzed in each experiment, and doxorubicin (**d**; 2 μM) was used as positive control

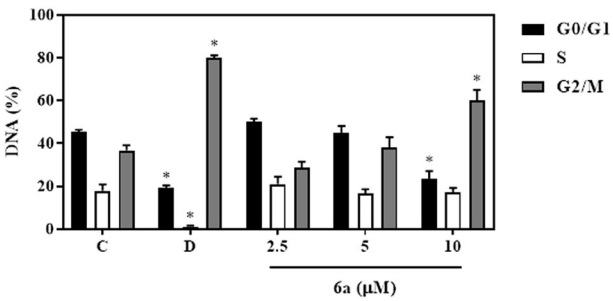

Fig. 7 Effect of chalcone **6a** on the DNA content of HCT-116 cells determined by flow cytometry using propidium iodate (PI) after 24 h of incubation. Data are presented as mean ± S.E.M. from three independent experiments performed in triplicate. *$p < 0.05$ compared with negative control (**c**) by ANOVA followed by Turkey's Test. Ten thousand events were analyzed in each experiment, and doxorubicin (**d**; 2 μM) was used as positive control

structure of the chalcone are capable of improving the in vitro effects against human cancer cells. In this context, chalcone N-(4′-[(E)-3-(3-nitrophenyl)-1-(phenyl)prop-2-en-1-one]) acetamide (**6a**) containing an amide group on ring A and a nitro group on ring B showed a strong and selective cytotoxic effect against HCT-116 cells and was able to induce cell death by apoptosis related to G2/M cell cycle arrest. These data provide us with the prospect of conducting studies on the specific mechanism of action of chalcone **6a** using human cancer cell-based assays.

Acknowledgements The authors thank the National Cancer Institute (Bethesda, MD, USA) for donating of all human tumor cell lines used in this study. CENAUREMN—Northeastern Center for the Application and Use of Nuclear Magnetic Resonance and EMBRAPA AGROINDÚSTRIA TROPICAL-Multiuser Laboratory of Natural Product Chemistry by obtaining the spectral data. Teixeira AMR also acknowledges financial support from the PQ/CNPq (Grant#: 3 05719/2018-1).

Compliance with ethical standards

Conflict of interest The authors declare that they have no conflict of interest.

Ethical approval This article does not contain any studies with human participants or animals performed by any of the authors.

Publisher's note Springer Nature remains neutral with regard to jurisdictional claims in published maps and institutional affiliations.

References

Abbas A, Naseer MM, Hasan A, Hadda TB (2014) Synthesis and cytotoxicity studies of 4-Alkoxychalcones as new antitumor agents. J Mater Environ Sci 5:281–292

Bhat BA, Dhar KL, Puri SC, Saxena AK, Shanmugavel M, Qazi GN (2005) Synthesis and biological evaluation of chalcones and their derived pyrazoles as potential cytotoxic agents. Bioorg Med Chem Lett 15:3177–3180

Boeck P, Bandeira Falcão CA, Leal PC, Yunes RA, Filho VC, Torres-Santos EC, Rossi-Bergmann B (2006) Synthesis of chalcone analogues with increased antileishmanial activity. Bioorg Med Chem 14:1538–1545

Bond MJ, Bleiler M, Harrison LE, Scocchera EW, Nakanishi M, G-Dayanan N, Keshipeddy S, Rosenberg DW, Wright DL, Giardina C (2018) Spindle assembly disruption and cancer cell apoptosis with a CLTC-binding compound. Mol Cancer Res 16:1361–1372

Cabrera M, Simoens M, Falchi G, Lavaggi ML, Piro OE, Castellano EE, Vidal A, Azqueta A, Monge A, de Ceráin AL, Sagrera G, Seoane G, Cerecetto H, González M (2007) Synthetic chalcones, flavanones, and flavones as antitumoral agents: biological evaluation and structure–activity relationships. Bioorg Med Chem 15:3356–3367

Corrêa R, Pereira MAS, Buffon D, dos Santos L, Filho VC, Santos ARS, Nunes RJ(2001) Antinociceptive properties of chalcones. Structure-activity relationships. Arch Pharm 334:332–334

De Campos-Buzzi F, Padaratz P, Meira VA, Corrêa R, Nunes JR, Cechinel-Filho V (2007) 4′-acetamidochalcone derivatives as potential antinociceptive agents. Molecules 12:896–906

de Campos-Buzzi F, Pereira de Campos J, Pozza Tonini P, Corrêa R, Augusto Yunes R, Boeck P, Cechinel-Filho V (2006) Antinociceptive effects of synthetic chalcones obtained from xanthoxyline. Arch Pharm 339:361–365

Das M, Manna K (2016) Chalcone scaffold in anticancer armamentarium: a molecular insight. J Toxicol 6:7651047

Di Carlo G, Mascolo N, Izzo AA, Capasso F (1999) Flavonoids: old and new aspects of a class of natural therapeutic drugs. Life Sci 65:337–353

Ducki S, Forrest R, Hadfield JA, Kendall A, Lawrence NJ, McGown AT, Rennison D (1998) Potent antimitotic and cell growth inhibitory properties of substituted chalcones. Bioorg Med Chem Lett 8:1051–1056

Guilherme AM, Jardim T, Guimaraes T, Maria do Carmo FR, Pinto BC, Cavalcanti KMF, Pessoa C, Gatto CC, Nair DK, Namboothiri INN, Junior ENS (2015) Naphthoquinone-based chalcone hybrids and derivatives: synthesis and potent activity against cancer cell lines. Med Chem Comm 6:120–130

Guo L, Zhang H, Tian M, Tian Z, Xu Y, Yang Y, Peng H, Liu P, Liu Z (2018) Electronic effects on reactivity and anticancer activity by half-sandwich N,N-chelated iridium (III) complexes. New J Chem 42:1–22

Hanahan D, Weinberg RA (2011) Hallmarks of cancer: the next generation. Cell 144:646–674

Hassan GS, El-Messery SM, Abbas A (2017) Synthesis and anticancer activity of new thiazolo[3,2-a]pyrimidines: DNA binding and molecular modeling study. Bioorg Chem 74:41–52

Jardim GAM, Guimarães TT, Pinto MCFR, Cavalcanti BC, Farias KM, Pessoa C, Gatto CC, Nair DK, Namboothir INN, Júnior ENS (2015) Naphthoquinone-based chalcone hubrids and derivatives: synthesis and potent activity against cancer cell lines. Med Chem Comm 6:120–130

Karaman İ, Gezegen H, Gürdere MB, Dingil A, Ceylan M (2010) Screening of biological activities of a series of chalcone derivatives against human pathogenic microorganisms. Chem Biodivers 7:400–408

Karthikeyan CN, Moorthy SH, Ramasamy N, Vanam S, Manivannan U, Karunagaran ED, Trivedi P (2015) Advances in chalcones with anticancer activities. Recent Pat Anticancer Drug Discov 10:97–115

Kepp O, Galluzzi L, Lipinski M, Yuan J, Kroemer G (2011) Cell death assays for drug discovery. Nat Rev Drug Discov 10:221–237

Kroemer G, Galluzzi L, Vandenabeele P, Abrams J, Alnemri ES, Baehrecke EH, Blagosklonny MV, El-Deiry WS, Golstein P, Green DR, Hengartner M, Knight RA, Kumar S, Lipton SA, Malorni W, Nuñez G, Peter ME, Tschopp J, Yuan J, Piacentini M, Zhivotovsky B, Melino G (2008) Classification of cell death: recommendations of the Nomenclature Committee on Cell Death 2009. Cell Death Differ 16:3–11

Lindamulage IK, Vu H-Y, Karthikeyan C, Knockleby J, Lee Y-F, Trivedi P, Lee H (2017) Novel quinolone chalcones targeting colchicine-binding pocket kill multidrug-resistant cancer cells by inhibiting tubulin activity and MRP1 function. Sci Rep 7:1–5

Martel-Frachet V, Keramidas M, Nurisso A, DeBonis S, Rome C, Coll JL, Ahcène B, Skoufias DA, Ronot X (2015) IPP51, a chalcone acting as a microtubule inhibitor with in vivo antitumor activity against bladder carcinoma. Oncotarget 6:14669–14686

Mosmann T (1983) Rapid colorimetric assay for cellular growth and survival: application to proliferation and cytotoxicity assays. J Immunol Methods 65:55–63

Nazir S, Ansari FL, Hussain T, Mazhar K, Muazzam AG, Qasmi ZU, Makhmoor T, Noureen H, Mirza B (2013) Brine shrimp lethality assay 'an effective prescreen': microwave-assisted synthesis, BSL toxicity and 3DQSAR studies-based designing, docking and antitumor evaluation of potent chalcones. Pharm Biol 51:1091–1093

Nowakowska Z (2007) A review of anti-infective and anti-inflammatory chalcones. Eur J Med Chem 42:125–137

Padaratz P, Fracasso M, De Campos-Buzzi F, Corrêa R, Niero R, Monache FD, Cechinel-Filho V (2009) Antinociceptive activity of a new benzofuranone derived from a chalcone. Basic Clin Pharm Toxicol 105:257–261

Pereira UA, Moreira TA, Barbosa LCA, Maltha CRA, Bomfim IS, Maranhão SS, Moraes MO, Pessoa C, Barros-Nepomuceno FWA (2016) Rubrolide analogues and their derived lactams as potential anticancer agents. Med Chem Comm 7:345–352

Prasad YR, Rani VJ, Rao AS (2013) In vitro antioxidant activity and scavenging effects of some synthesized 4'-aminochalcones. Asian J Chem 25:52–58

Rossette MC, Moraes DC, Sacramento EK, Romano-Silva MA, Carvalho JL, Gomes DA, Caldas H, Friedman E, Bastos-Rodrigues L, De Marco L (2017) The in vitro and in vivo antiangiogenic effects of Flavokawain B. Phytother Res 31:1607–1613

Santos MB, Pinhanelli VC, Garcia MAR, Silva G, Baek SJ, França SC, Fachim AL, Marins M, Regasini LO (2017) Antiproliferative and pro-apoptotic activities of 2- and 4-aminochalcones against tumor canine cells. Eur J Med Chem 138:884–889

Shankaraiah N, Nekkanti S, Brahma UR, Praveen Kumar N, Deshpande N, Prasanna D, Senwar KR, Jaya Lakshmi U (2017) Synthesis of different heterocycles-linked chalcone conjugates as cytotoxic agents and tubulin polymerization inhibitors. Bioorg Med Chem 25:4805–4816

Zingales SK, Moore ME (2016) Design and Synthesis of (2-(furanyl) vinyl)-1-tetralone chalcones as anticancer agents. Der Pharma Chem 8:40–47

Tristão TC, Campos-Buzzi F, Cruz RCB, Filho VC, Cruz AB (2012) Antimicrobial and citotoxicity potential of acetamido, amino and nitrochalcones. Arzneimittelforschung 62:590–594